Design and Simulation 4-Channel Demultiplexer Based on Photonic Crystals Ring Resonators

Reza Ghavidel Barsary [1], Alireza Andalib [2], Hamed Alipour-Banaei [3]

[1]Department of Electrical Engineering, Ahar Branch, Islamic Azad University, Ahar, Iran
Email: Rezaghavidelbarsary@yahoo.com

[2,3]Department of Electrical Engineering, Tabriz Branch, Islamic Azad University, Tabriz, Iran
Email: Andalib@iaut.ac.ir
[3]Email: H_alipour@tabrizu.ac.ir

ABSTRACT

In this paper, a new design of demultiplexer based on two-dimensional photonic crystal ring resonator is proposed. The structure is made of a hexagonal lattice of silicon rods with the refractive index 3.46 in coefficient of air with refractive index 1. The transmission efficiency and Quality factor for our proposed demultiplexer, respectively, are more than 65% and 1600. The normalized transmission spectra of the photonic crystal ring resonator are taken using Two-dimensional (2D) Finite Difference Time Domain (FDTD) method. The photonic band gap is calculated by Plane Wave Expansion (PWE) method.

KEYWORDS: Demultiplexer, Photonic crystal, Quality factor, Ring resonator

1. INTRODUCTION

Photonic crystals are new structures , that in recent years have attracted much attention due to their optical properties and potential that these reasons in the circuit design of optical and telecommunication networks have many applications. Photonic crystals are artificial structures which consist of periodic arrays of dielectric materials [1-3]. Photonic crystals can light waves in the micrometer range that is very small, incarcerate or conduct [2,4] . The most important feature of these structures is the photonic band gap. The photonic band gap to a region of the photonic crystal band structure is called that in this area, no wavelength is not allowed to release into the crystal [5-7] . By using the defects effects in photonic crystal structures, periodicity and photonic band gap have been broken, and the light is entered to a region of photonic band gap and this could lead to the design of optical devices be based photonic crystals such as optical demultiplexers [8] and optical filters [9], and etc.

Ring resonators photonic crystal due to the coefficient of the high quality and the nature of their single mode ring and flexibility have a choice of high spectral resolution that provides optical design types

of electronic devices [10]. In communication systems for optimal utilization of transmission channel capacity multiplex operation, and demultiplex signals occur. Demultiplexers are useful and essential elements of photonic integrated circuits which separate wavelengths multiplexed signals. In this paper, we designed a demultiplexer four-channel by using four ring resonators two-dimensional photonic crystal with the new structure. Also for simulation of electromagnetic wave propagation in time domain is used finite difference method in 2D time-domain (2D-FDTD) and to calculate the photonic band gap the plane wave expansion method (PWE) is used.

2. STRUCTURE DESIGN

There are several methods for the design of optical demultiplexers , according to the properties of ring resonators, the ring resonators can be a good option for the design of optical demultiplexers. From the main and important features of optical demultiplexers are for optical telecommunications systems, polarization-independent, crosstalk, high-quality spatial resolution and compression, allowing integration. Photonic crystals are with two topologies that first of them, contains a dielectric layer which air holes are introduced to periodically periodic, and second consists of dielectric rods . embedded on bed of air . In this paper, we designed the structure in Figure 1, based on 2D photonic crystals, of the silicon rods with refractive index 3.46 , in the field of air with refractive index 1 , is located . The number of rods in the x and z directions are respectively, 34 and 31. Lattice constant of the entire structure (a) is equal to 583 nm,

and the radius of each of the rods is equal to 115 nm .

Figure.1. Shows our proposed demultiplexer.

This structure consists of two photonic band gap in TM mode and one photonic band gap in TE band . Normalized frequency of the first photonic band gap of above corresponds to TE mode is equal to $0.87631 \geq a/\lambda \geq 0.82264$, which corresponds to a wavelength range from 0.665 to 0.708 micrometer . The second photonic band gap that is related to the TM mode, the normalized frequency is $0.59349 \geq a/\lambda \geq 0.56915$ and the wavelength range is from 0.982 micrometer to 1.024 micrometer and the last photonic band gap that is related to the TM mode, the normalized frequency is $0.45056 \geq a/\lambda \geq 0.27753$ and the wavelength range is from 1.293 micrometer to 2.1 micrometer. Figure.2 shows the band structure of the photonic crystal that is in TM polarization mode. Our structure consists of several parts which includes a waveguide that is in the middle of the

structure, and the structure in approximation has divided into two halves. Our structure also includes 4 rings that have a new structure. There are also four smaller waveguides that are located above each ring. Each ring be in the middle of the intermediate waveguide and a small waveguide.
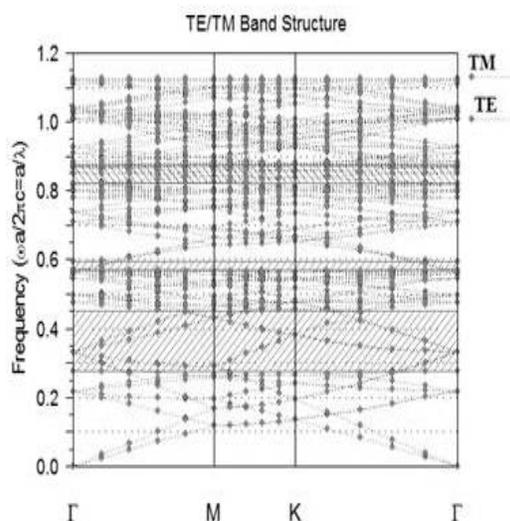
Figure.2. Shows the band structure

We construct a new ring resonator as shown in Figure.3, including 6 rods of the scatter that the radius of each ring is different that have been shifted as much as 25% of its original location and scatters radius of the right ring above the intermediate waveguide is equal to 56.69 nm and scatters radius of the left ring above the intermediate waveguide is equal to 55.15 nm and scatters radius of the right ring down the intermediate waveguide is equal to 56.37 nm and scatters radius of the left ring down the intermediate waveguide is equal to 56.09 nm. There are 2 rows of ring inner rods which rods that are blue, as much as 25% are shifted of its original

location . Different in scatter rods of each ring causes different wavelengths.
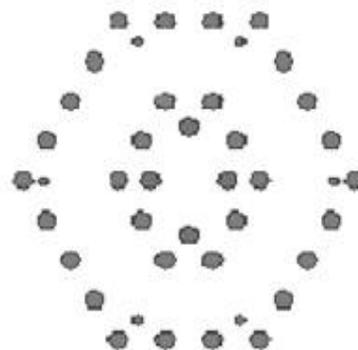
Figure.3. Ring structure used in demultiplexer

3. SIMULATION RESULTS

Gaussian stimulation signal to the input port (A), that is the intermediate waveguide, is applied . The signal output by the time monitors, that is located in the output port (B, C, D, E), is to be recorded . Figure. 4 shows the normalized transmission spectrum of 4-channel demultiplexer that is based on photonic crystal ring resonator. As shown in Figure.4 it can be seen for output port B, the transmission efficiency is equal to 67.93% and the quality coefficient is equal to 1868.27. For output port E, the transmission efficiency is equal to 83.23% and the quality coefficient is equal to 1918.6. For output port C, the transmission efficiency is equal to 93.53% and the quality coefficient is equal to 2023.48 and for output port D, the transmission efficiency is equal to 88.02% and the quality coefficient is equal to 1668.78.
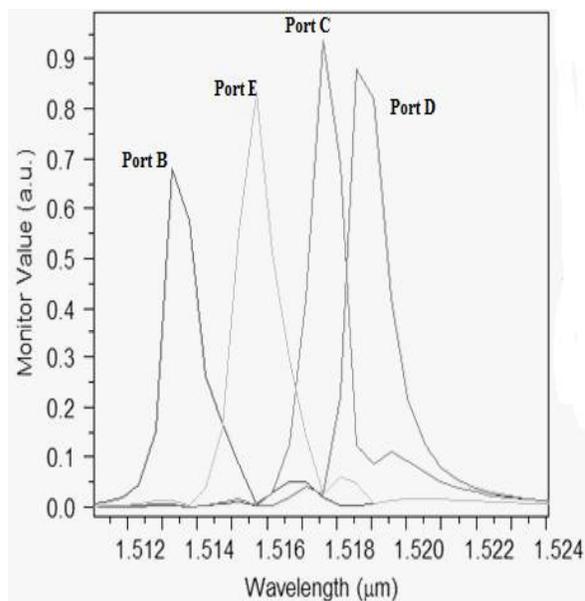
Figure.4. Shows the normalized transmission spectrum of 4-channel demultiplexer

Audition value port of D to port C is calculated equals to -16.49 dB and total audition value of port C to port D equals to -26.85 dB and total audition value port B to port E equal to -32.38 dB. This value for the other ports is equal to zero.

4. CONCLUSIONS

In this paper, we design an optical demuliplexer based on photonic crystal ring resonator. For output port C the transmission efficiency is equal to 93.53% and the quality coefficient is equal to 2023.48. For 4 channel we have, the transmission efficiency and the quality factor of this demultiplexer, more than 65% and 1600 respectively. This approach represents a novel technique for creating high-Q demultiplexer that furthermore opens the possibility of the photonic integrated circuits.

REFERENCES

[1] J D Joannapolous, R D Meade and J N Winn, Photonic crystals: Molding the flow of light, Princeton University Press, New Jerse, 08540, 1995.

[2] K Sakoda, Optical properties of photonic crystals, Springer, Berlin, 2001.

[3] YOGITA KALRA and R K SINHA, "Photonic band gap engineering in 2D photonic crystals," PRAMANA journal of physics" Vol.67, 1155-1164 , 2006.

[4] Hadjira Badaoui1, Mohammed Feham1 and Mehadji Abri," Photonic-Crystal Band-pass Resonant Filters Design Using the Two-dimensional FDTD Method," IJCSI International Journal of Computer Science Issues, Vol. 8, 127-132 ,2011.

[5] S-I. Takayama, H. Kitagawa, Y. Tanaka, T. Asano and Susumu Noda, "Experimental demonstration of complete photonic band gap in two-dimensional photonic crystal slabs," Appl.Phys. Lett., vol. 87, Article no. 061107, 2005.

[6] Nobuhiko Susa, "Large absolute and polarization-independent photonic band gaps for various lattice structures and rod shapes," J. OF Appl. Phys., vol. 91, no. 6, pp.3501-3510, March ,2002.

[7] Z.-Y. Li, "Large absolute band gap in 2D anisotropic photonic crystals," Phys. Rev. Lett., vol. 81, no. 12, pp. 2574-2577, Sept. 1998.

[8] A. Ghaffari,et al., "Heterostructure wavelength division demultiplexers using photonic crystal ring resonators," Opt. Commun.vol. 281, 4028–4032, 2008.

[9] M. David, et al., "T-Shaped channel drop filters using photonic crystal ring resonators," Physica E,vol. 40, pp. 3151–3154, 2008.

[10] M.Y.Mahmoud,GH.Massou,A.Taalbi and Z.M.Chekroun,"Optical channel drop filters based on photonic crystal ring resonators," Optics Communications 285,368–372., 2012.

Finite Element Method Application in Analyzing Magnetic Fields of High Current Bus Duct

Seyed Mohamad Hasan Hoseyni[1,] Vahid Montaghemi[2]

[1] Department of Power System Engineering, Tehran South Branch of Islamic Azad University, Tehran, Iran
Email:smhh110@yahoo.com

[2] Department of Power System Engineering, Tehran South Branch of Islamic Azad University, Tehran, Iran
Email:vahidmontaghami@yahoo.com

ABSTRACT

The goal of paper is to present the magnetic field calculations in high current bus ducts. Finite element method is used to do this. Bus ducts under study have figure such as circle area. The calculations will be using mathematical relations, meshed geometric shape and analyzing them. Geometric mean will help us to determine the value of magnetic field. COMSOL software is applied for simulation studies. Calculations have been analyzed in three phase state and also, simulations are implemented into the three dimensional position. Demonstration procedure and numerical calculations are used for presentation the front of view of bus duct. Skin effect and connection configuration between bus ducts are considered in the calculations. Aforementioned method can be used in the magnetic fields analyzing in transmission lines and electrical energy link which consist of insulator, easily. Typical bus duct which is applied in simulation studies produced by a pars generator corporation, it has been installed in Ardebil substation.

KEYWORD: High Current Bus Duct, Magnetic Field, Meshed-Finite Element, Gas Insulated Lines (GIL)

1) INTRODUCTION

Usually, high level current systems use bus duct to transfer electrical energy. These systems in the form of single or three phases can be located in the isolated cabinet. If, value of current is very high then, three parallel single phase line will be used. Also, geometric shapes of bus ducts are different. The connected Square figures in the form of latticed or circular are different type of geometric figures. Most common and best state for high level current bus ducts will be the use of circular figures. Usually, bus ducts are constructed of copper or aluminum. Bus duct configuration with regarded to equipment position will be vertically or horizontally. Often, location of this equipment is between generators and transformers connection. With regard to terminal voltage on the generator output is between 5kv to 30kv, therefore, current value in this location will be very high, between 1kA to 30kA approximately. These equipments are more applicable in hydropower plants because of generator installation into the hydro tunnels path [1-2]. The usage of Gas Insulated transmission Line (GIL) technology

is very appropriate for a short time and long time states [3]. Rated voltage and current of these lines can be between 20kV to 530kV and 1kA to 30kA, respectively. Insulator usually, is composed of 80% nitrogen and 20% sulfate hex florid, which is introduced N2-SF6 and or SF6 gas is applied. Use of GIL technology has been as a favorite technology (Transfer electrical energy to short and long distances). Recently, very modern projects have scheduled for more use of GIL technology in the European and china. The GIL systems are applied by different types, for example, passed due to the ground, passed due to tunnel or channel, passed due to environment. Less transfer losses, high reliability, low capacitive load and environment with appropriate quality might be considered as advantages of the use of this technology. Copper or aluminum conductors, which are used in bus duct construction, with regard to geometric shape will have variable range between 1m to multiple m. Passed, induced and eddy currents into the bus ducts will cause to magnetic field generation with high values. These fields have an effect on self bus ducts, in addition to will have a bad effect on equipments and proximate humans. Indeed, bus duct singly is an Electromagnetic Interference source. EMI is considered as a basic menace for sensitive equipments which are installed in power plants. Consider of importance of subject of electromagnetic fields in bus ducts, in this paper present an appropriate method of calculations. This is based on the Finite Element method (FEM). Commercial software is produced in this domain, which will help us in improving in simulation performances. One of them is COMSOL multi physic software. Magnetic field analyzing in front of view state is considered for three phase networks. Also, simulation has implemented by three dimensional figure in a COMSOL software environment.

2) MATHEMATICAL MODEL

A current path system with insulator is shown in figure (1). This presentation is top view of equipment and circuit. To calculation the exact field distribution in bus duct, all cases which is related to physics of subject should be considered. These cases consist of: (1) Value of passed current through a conductor, (2) Resistance value and permeability in each filament which is independent from current value. (3) Mutual effects between phases with together. Filament Method is discussed for modeling in the reference [12]. Aforementioned method is recognized as one of the best methods in high voltage cables and high level current bus duct. Based on this method each bus is divided to multiple filaments (Nc). Insulator and other point will divide to Ns filaments. Finally, for a three phase model will have N=3Nc+3Ns filament. Use of meshed method in finite element is based on these rules. Therefore, it can be used in smaller mesh for more exact calculations. Thus, the relation between plates and lack of uniformity are not considered [1].

Figure.1: Bus duct network in a power plant

The equation is governed on the system will be according to bellow form (1).

$$\{V\} = [Z]\{I\}$$

(1)

{V} in relation (1) will express voltage vector in close loop between source and load. Matrix [z] is creation impedance. {I} is related to current matrix in close loop system. During impedance matrix building, it will need to geometric mean distance (GMD). Calculation this value will be very complicated. Value of GMD related to each filament (ith) will find by using relation (2). In relation (2), ai and bi will be dimension values of surface area.

$$d_{ii} = 0.22355 \cdot (a_i + b_i)$$

(2)

Also, GMD between each pair of bus duct system is given as a geometric distance among central points, for example, GMD between ith and kth filament is calculated by relation (3): x and y, which are related to position center of filaments.

$$d_{ik} = \sqrt{(x_i - x_k)^2 + (y_i - y_k)^2}$$

(3)

Introduced Bus duct system in figure (1) has earth system that will be shown by equation (4).

$$
\begin{Bmatrix} \overline{V}_A \\ \overline{V}_B \\ \overline{V}_C \\ - \\ 0 \\ 0 \\ 0 \\ - \\ 0 \end{Bmatrix}
=
\begin{bmatrix}
Z_{AA} & Z_{AB} & Z_{AB} & & 1 & \\
Z^T_{AB} & Z_{BB} & Z_{BC} & Z_{CS} & \vdots & \\
Z^T_{AC} & Z^T_{BC} & Z_{CC} & & 1 & \\
-- & -- & -- & -- & - & \\
& Z^T_{CS} & & Z_{SS} & \vdots & \\
& & & & 0 & \\
-- & -- & -- & -- & - & \\
1 & \cdots & 1 & 0 \cdots 0 & 0 &
\end{bmatrix}
\times
\begin{bmatrix} I_1 \\ \vdots \\ \vdots \\ I_N \\ - \\ \Delta \overline{V} \end{bmatrix}
$$

(4)

Also, there are following relations:

$$\overline{V}_A = \{1\}^T . \overline{V}_{L1}$$

(5)

$$\overline{V}_B = \{1\}^T . \overline{V}_{L2}$$

(6)

$$\overline{V}_C = \{1\}^T . \overline{V}_{L3}$$

(7)

In these relations, $\{1\}^T$ is as an identical transpose matrix. Matrix VL shows network voltage. Also, internal impedance matrix, the impedance between filaments and impedance between network and earth are shown on above relations

It should be noted that, resistance in each phase and network part is a function of temperature. In this paper for means of simplification, it is assumed that source side and load side are ideal. With previous definition and relations, we can study system in a short circuit condition and also, load balance and unbalance conditions [4-7]. In equation (4), we can see that, there are N+1 known parameters while, there are many unknown variables (3Ns+3Nc). In addition to potential difference also will be part of problem variables. Determining the current distribution

in the system and calculating the proximity effect with a bus duct to other equipments by using this method will be efficient. For analyzing field distribution in bus duct surrounding, geometry is presented in figure (2) will be used. Bus duct and surrounding space are shown in figure (2).

Figure.2: vector coordinates to calculate magnetic field

One typical point such as M in figure (2), for magnetic field caused by special point of bus duct such as T will be calculated. When these calculations are performed to all points of space and bus duct, it can be seen magnetic field as identically. Distance vectors and current have been depicted by polar coordinates. Different variables will define based on figure (2):

$$\xi_k = (x_k - x_i).\sin\delta_i - (y_k - y_i).\cos\delta_i$$
(8)

$$\eta_k = (x_k - x_i).\cos\delta_i + (y_k - y_i).\sin\delta_i$$
(9)

By use of bellow relationships the tangent and vertical parts of magnetic field will be known with polar coordinates.

$${}^{t}H_{ki} = {}^{\xi}H_{ki}.\cos(\vartheta_k - \delta_i) + {}^{\eta}H_{ki}.\sin(\vartheta_k - \delta_i)$$
(10)

$${}^{r}H_{ki} = {}^{\xi}H_{ki}.\sin(\vartheta_k - \delta_i) + {}^{\eta}H_{ki}.\sin(\vartheta_k - \delta_i)$$
(11)

By use of busaver rules in electromagnetic discussion and defined relations based on figure (2) the severity of magnetic field in same direction of ξ axis will be as following relation (12). Similarly, by use of busaver rules the severity of magnetic field in same direction of η axis will find with relation (13).

$$
{}^{\xi}H_{ki} = -\frac{\overline{I}_i}{2\pi.a_i.b_i}.\left[\frac{1}{2}\left(\zeta_k + \frac{a_i}{2}\right).\ln\frac{\left(\eta_k + \frac{b_i}{2}\right)^2 + \left(\zeta_k + \frac{a_i}{2}\right)^2}{\left(\eta_k - \frac{b_i}{2}\right)^2 + \left(\zeta_k + \frac{a_i}{2}\right)^2} - \right.
$$

$$
\frac{1}{2}\left(\zeta_k - \frac{a_i}{2}\right).\ln\frac{\left(\eta_k + \frac{b_i}{2}\right)^2 + \left(\zeta_k - \frac{a_i}{2}\right)^2}{\left(\eta_k - \frac{b_i}{2}\right)^2 + \left(\zeta_k - \frac{a_i}{2}\right)^2} +
$$

$$
\left(\eta_k + \frac{b_i}{2}\right).\left(a\tan\frac{\zeta_k + \frac{a_i}{2}}{\eta_k + \frac{b_i}{2}} - a\tan\frac{\zeta_k - \frac{a_i}{2}}{\eta_k + \frac{b_i}{2}}\right)
$$

$$
\left. -\left(\eta_k - \frac{b_i}{2}\right).\left(a\tan\frac{\zeta_k + \frac{a_i}{2}}{\eta_k - \frac{b_i}{2}} - a\tan\frac{\zeta_k - \frac{a_i}{2}}{\eta_k - \frac{b_i}{2}}\right)\right]
$$

(12)

$$^{\eta}H_{ki} = -\frac{\bar{I}_i}{2\pi.a_i.b_i}.[\frac{1}{2}\left(\eta_k+\frac{a_i}{2}\right).\ln\frac{\left(\xi_k+\frac{b_i}{2}\right)^2+\left(\eta_k+\frac{a_i}{2}\right)^2}{\left(\xi_k-\frac{b_i}{2}\right)^2+\left(\eta_k+\frac{a_i}{2}\right)^2}-$$

$$\frac{1}{2}\left(\eta_k-\frac{a_i}{2}\right).\ln\frac{\left(\xi_k+\frac{b_i}{2}\right)^2+\left(\eta_k-\frac{a_i}{2}\right)^2}{\left(\xi_k-\frac{b_i}{2}\right)^2+\left(\eta_k-\frac{a_i}{2}\right)^2}+$$

$$\left(\xi_k+\frac{b_i}{2}\right)\left(a\ \tan\frac{\xi_k+\frac{a_i}{2}}{\xi_k+\frac{b_i}{2}}-a\ \tan\frac{\eta_k-\frac{a_i}{2}}{\xi_k+\frac{b_i}{2}}\right)$$

$$-\left(\xi_k-\frac{b_i}{2}\right)\left(a\ \tan\frac{\eta_k+\frac{a_i}{2}}{\xi_k-\frac{b_i}{2}}-a\ \tan\frac{\eta_k-\frac{a_i}{2}}{\xi_k-\frac{b_i}{2}}\right)]$$

(13)

Total value of magnetic flux density is calculated by summing all partial values according to the relations (14) and (15).

$$^{t}\overline{H}_k = \sum_{i=1}^{N}{}^{t}H_{ki}$$

(14)

$$^{r}\overline{H}_k = \sum_{i=1}^{N}{}^{r}H_{ki}$$

(15)

Ampere rule can be used for presenting the phasor of severity of magnetic field and to calculate the total value of magnetic flux density according to the relation (16).

$$H_k = \sqrt{\left(\left|{}^{t}H_K\right|^2+\left|{}^{r}H_K\right|^2\right)}$$

(16)

The value of B by use of H value according to the relation (17) can be calculated.

$$B_k = \mu_0.H_k$$

(17)

3) **Simulation and Numerical Studies**

A typical bus duct system for simulation studies is pars generator corporation product which, it has been installed on Ardebil substation. The test system is shown in figure (3).
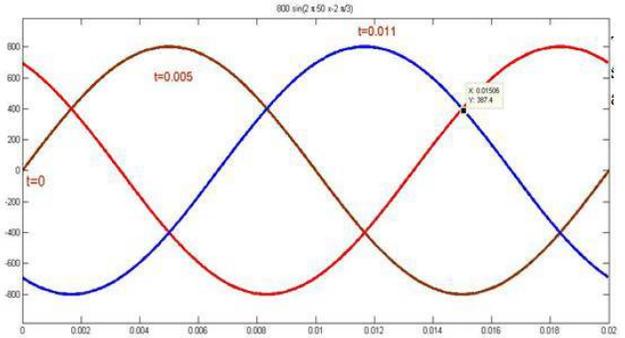
Figure.3: bus duct under studies

Effective level and impulse of bus duct voltage are equal to 38kV and 95kV, respectively. Rated current and power loss in each conductor are equal to 800A and 12W/m. Instantaneous current capability is equal to 500kA. Design of environment temperature for bus duct is 44°c. Permissible conductor temperature and insulator are 105°c and 80°c, respectively. The value of load resistance is 100Ω. Also, earth resistance has been neglected. Test network is simulated in the COMSOL environment by filament method [8]. The calculation will conduct with regard to 800A current in each phase. To achieve this goal, it is necessary that critical conditions and times which three phase composition create a bad condition to bus duct and surrounding space, are analyzed. Three phase curve with 800A will be according to figure (4).
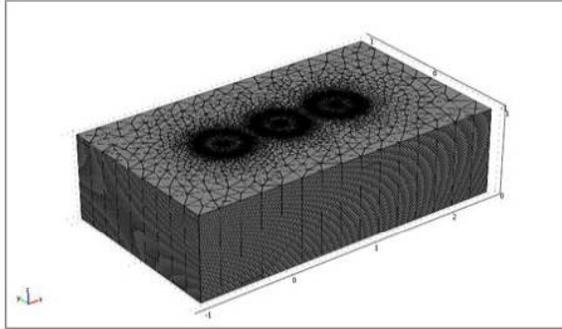
Figure.4: the curve of bus duct three phase current

Critical and sensitive values to simulation studies have been shown in the table (1).

Table 1: bus duct current values for different time

I_T	I_S	I_R	t
-692.8	692.8	0	0
-400	-400	800	0.005
800	-400	-400	0.011

With regard to that, there is current density requirement in calculations, it will compute based on the values of current and lateral surface area of bus duct according to the table (2).

Table 2: value of current density for different current

692.8	400	800	I
2450.7	1415	2829.9	J

By use of the meshed method for bus duct, the system will convert in many separate filaments and number of meshes should increase where is near to bus duct. In the test system total number of meshes will equal to 32406.
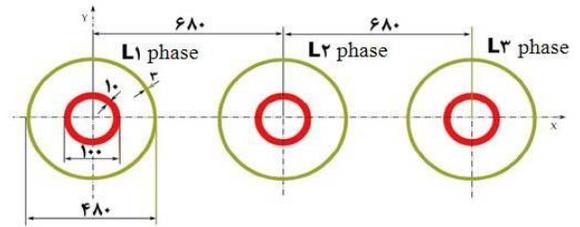
Figure.5: meshed environment in three dimensional simulation
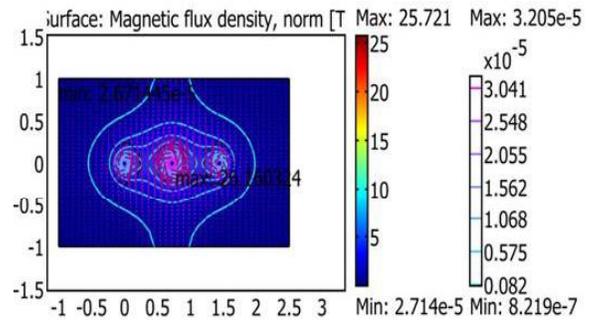
Figure.6: flux density and vectors of magnetic field
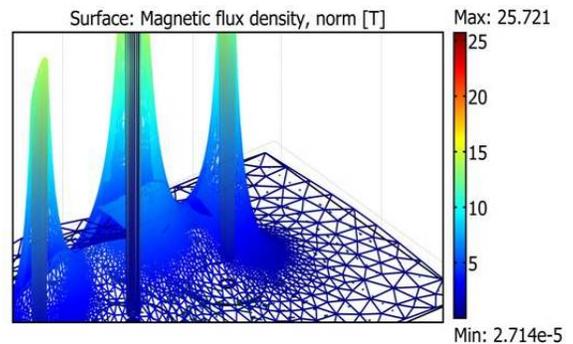
Figure.7: magnetic flux density with three dimensional representation
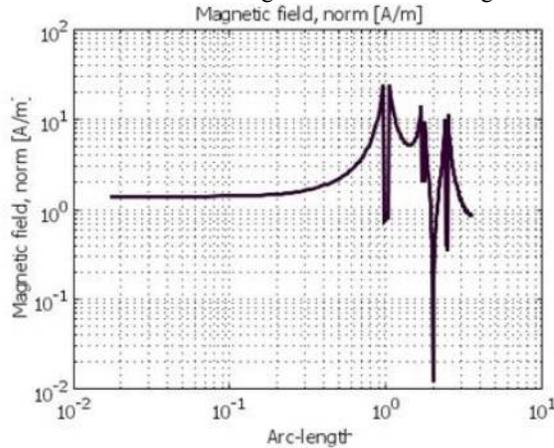
Figure.8: logarithmic representation of magnetic field based on distance of surrounding

By considering to earth system, the current value of earth system will be equal to 1.2A. System power loss for different parts of system is according to the table (3). Also, the magnetic flux density profile in two states (1m and 0.5m distance), is shown in figure (9).

Table 3: power losses representation in different part of system

Power losses	Losses (W/m)		
	R	S	T
System conductors	11	11	11.
shell	12	12.	13
Total	0	73.7	0
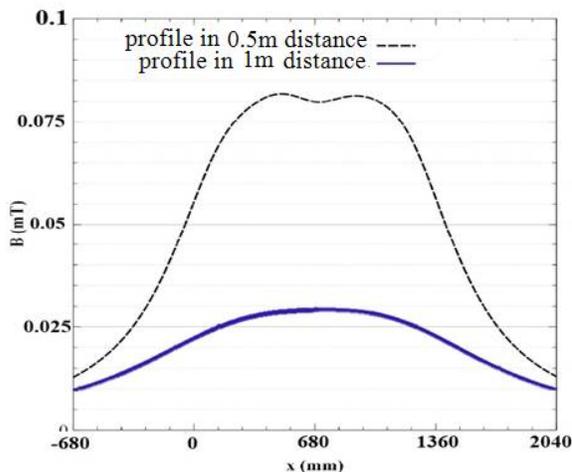
Figure.9: magnetic flux density profile in two states (1m and 0.5m distance)

If both sides of bus duct are connected to earth system, value of flux density will be about 0.031623mT while, if one side of bus duct is connected to earth system and other side remain free, therefore maximum of flux density will equal to 0.5mg.

4) CONCLUSION

There are different factors on the amount of bus duct undesirable effect such as total power losses, network over voltages and magnetic field on proximity equipments. Better conditions will provide when, power losses and induced voltage on plate shell are minimized. Use of parallel bus duct in single phase causes to decrease in magnetic field which, decrement amount should be analyzed. Also, under real dimension and geometric shape conditions, calculation of electromagnetic field is very complicated therefore use of computational software in this field is an approach to overcome this problem. Numerical method and finite element are most common method in this software. Filament method as one of the best method has been proposed in this paper.

REFERENCES

[1] Benato, R,"Gas Insulated Transmission Lines in Railway Galleries", IEEE Trans. Power Deliv.2005, 20, pp: 704–709.

[2] Piatek, Z., Kusiak, D., Szczegielniak, T.,"Electromagnetic Field and Impedances of High Current Busducts", In Proceedings of the International Symposium Modern Electric Power Systems (MEPS), Wroclaw, Poland, 20–22, Sep 2010.

[3] Surutka, J. "Electromagnetics, 2nd ed.; Engineering Books", Belgrade, Yugoslavia, 1966 (in Serbian).

S.M.H.Hoseyni, V.Montaghemi: Finite Element Method Application in Analyzing Magnetic …

[4] Sarajčev, P., Goić, R."Power loss computation in high-current generator bus ducts of rectangular cross-section", Electric Power Compon. Syst. 2010, 38, 1469−1485.

[5] K. B. Madhu Sahu and J. Amarnath," Effect of Various Parameters on the Movement of Metallic Parameters in a Single Phase Gas Insulated Bus Duct With Image Charges and Dielectric Coated Electrodes", ARPN Journal of Engineering and Applied Sciences, VOL. 5, NO. 6, JUNE 2010.

[6] K.B. Madhu Sahu and J. Amarnath," Movement of metallic particle contamination in a gas insulated busduct under dielectric coated enclosure with electromagnetic field effect", Indian Journal of Science and Technology, Vol. 3 No. 7, July 2010.

[7] L. Rajasekhar , D. Subbarayudu, and J. Amarnath," Metallic Particle Motion in A Single Phase Gas Insulated Busduct Under the Influence of Power Frequency Voltages", International Journal of Electronic and Electrical Engineering, Volume 3, Number 12010.

[8] http://www.comsol.com.